Aus dem Fachbereich Medizin

der Johann Wolfgang Goethe-Universität

Frankfurt am Main

betreut an der

Orthopädischen Universitätsklinik Friedrichsheim

Direktorin: Prof. Dr. Andrea Meurer

Time course of traumatic neuroma development/role of electrical stimulation

in inhibition of neuroma formation in a rat limb amputation model

Dissertation

zur Erlangung des Doktorgrades der Medizin

des Fachbereichs Medizin

der Johann Wolfgang Goethe-Universität

Frankfurt am Main

vorgelegt von

Lukáš Pindur

aus Český Těšín (Tschechische Republik)

Frankfurt am Main, 2020

Dekan: Prof. Dr. Stefan Zeuzem

Referent: Prof. Dr. John H. Barker

Korreferent/in: Prof. Dr. Dirk Günter Henrich

Tag der mündlichen Prüfung: 03.06.2020

Table of Contents

List of Figures

List of Tables

1. Summary

Limb stump pain after amputation, due to sensitized neuromas, is a common condition that can cause a great deal of suffering in affected patients. Treatment is difficult, requiring a multidisciplinary approach that is often unsatisfactory. One treatment used to mitigate pain is electrical stimulation (EStim), administered using several different therapeutic approaches. The research described in this dissertation sought to characterize changes in peripheral nerve morphology, and neuroma formation, following limb amputation, with an eye toward developing better treatment strategies, that intervene before neuromas are fully formed. Another focus of this study was to evaluate the effect EStim has on changes in peripheral nerve morphology, and neuroma formation, following limb amputation.

Right forelimbs of 42 male Sprague Dawley rats were amputated. At 3, 7, 28, 60 and 90 days post amputation (DPA) 6 limb stumps, in each group, were harvested and changes in peripheral nerve morphology, and neuroma formation were measured. In addition, limb stumps of 6 EStim treated, 6 sham-treated (deactivated EStim devices), and 6 non-treated rats were harvested at 28 DPA.

Analysis revealed six distinct morphological characteristics of peripheral nerves during nerve regrowth and neuroma development; 1) normal nerve, 2) degenerating axons, 3) axonal sprouts, 4) unorganized bundles of axons in connective tissue, 5) unorganized axon growth into muscles, and 6) unorganized axon growth into fibrotic tissue (neuroma). At the early stages (3 & 7 DPA), normal nerves could be identified throughout the limb stump tissues and small areas of axonal sprouts were present near the distal tip of the stumps. Signs of degenerating axons were evident from 7 to 90 DPA. From day 28 on, variability of nerve characteristics, with signs of unorganized axon growth into muscle and fibrotic tissue, and neuroma formation, became visible in multiple areas of stump tissue. These pathological features became more evident at 60 and 90 DPA. EStim treated stumps revealed neuroma formation in 1 out of 6 animals, whereas in sham and controls, neuroma formation was seen in 4 out of 6 stumps respectively.

We were able to identify 6 separate histological stages of peripheral nerve regrowth and neuroma formation over 90 days following amputation. Axonal regrowth was observed as early as 3 DPA, and signs of unorganized axonal growth and neuroma formation were evident by 28 DPA. Our observations suggest that EStim-based treatment and/or other prevention strategies might be more effective if administered in the initial dynamic stages of neuroma development.

1.1 Zusammenfassung

Stumpfschmerz nach Extremitätenamputation infolge eines symptomatischen Neuroms ist häufig und kann die Lebensqualität der Patienten erheblich beeinträchtigen. Die Therapie ist kompliziert und bedarf einer interdisziplinären Zusammenarbeit, trotzdem bleiben die Ergebnisse nicht selten unbefriedigend. Einer der Therapieansätze, die Schmerzen zu lindern, basiert auf der Anwendung einer elektrischen Stimulation in verschiedenen Formen. Das Ziel dieser Dissertation war es, die morphologischen Veränderungen der peripheren Nerven und der Neurome nach der Extremitätenamputation zu beschreiben mit Blick auf die Entwicklung besserer Therapiestrategien der Neuromprophylaxe. Ein nächstes Ziel der Studie war es, die Rolle der elektrischen Stimulation mittels Gleichstrom in der Verhinderung der Neuromentwicklung zu beurteilen.

Rechte Vordergliedmaßen von 42 Sprague Dawley Ratten wurden amputiert. Am 3., 7., 28., 60 und 90. Tag nach der Amputation (TnA) wurden in jeder Gruppe 6 Extremitätenstümpfe gesammelt und die Veränderungen der Morphologie der peripheren Nerven und der Neuromentwicklung ausgewertet. Extremitäten von 6 Tiere behandelt mit einer elektrischen Stimulation, von 6 „sham" Tiere behandelt mit einem inaktivierten Stromgeber und von 6 Tieren der Kontrollgruppe wurden am 28 TnA gesammelt.

Sechs verschiedene morphologische Merkmale der peripheren Nerven während der Nervenregeneration und Neuromentwicklung wurden histologisch analysiert: 1) ein normaler Nerv, 2) ein degenerierender Nerv, 3) Axonaussprossungen, 4) nicht organisierte Axonfaszikeln im Bindegewebe, 5) nicht organisierte Axonfaszikeln im Muskelgewebe, 6) nicht organisierte Axonfaszikeln im fibrotischen Gewebe (Neurom). Während der Frühstadien (3 und 7 TnA) konnten normale periphere Nerven in der ganzen Gliedmaße und Axonaussprossungen nah am distalen Stumpfanteil beobachtet werden. Die degenerierenden Axone wurden vom 7 bis 90 TnA dokumentiert. Ab dem 28 TnA zeigten sich variable morphologische Merkmale mit Zeichen des nicht organisierten axonalen Wachstums im Muskel- und fibrotischen Gewebe sowie Neurome in multiplen Stumpfanteilen. Diese

pathologischen Merkmale wurden evidenter am 60 und 90 TnA. In den elektrisch stimulierten Stümpfen konnte in 1 von 6 Ratten ein Neurom beobachtet werden, während sich bei 4 von 6 Tieren in der Kontroll- und der „sham"-Gruppe Neurome zeigten.

Wir konnten 6 verschiedene histologische Stadien der peripheren Nerven und Neuromentwicklung nach der Amputation der vorderen Extremität beschreiben. Axonaussprossungen zeigten sich bereits am 3. TnA, die Zeichen des nicht organisierten axonalen Wachstums sowie eines wahren Neuroms hingegen ab dem 28 TnA. Ausgehend von diesen Beobachtungen schlussfolgern wir, dass die strom-basierten oder anderen Therapiestrategien der Neurombehandlung/-prävention effektiver sein können, wenn sie in den Initialstadien der Neuromentwicklung eingeleitet werden.

2. Introduction

2.1 Post-amputation neuroma formation

In 2005, an estimated 1.6 million persons suffered limb loss in United States alone, and this figure is expected to triple by 2050[1]. The most common causes of limb amputation are vascular diseases and trauma, with malignancy-related amputations being relatively rare[2]. Limb amputation is a devastating condition that results in both functional and psychological disability in affected patients[3,4]. One of the most common complaints for which amputee patients seek treatment is pain. There are two major types of postamputation pain, phantom and residual limb pain. While phantom limb pain is experienced as a painful sensation in the area of the lost limb or limb part, residual limb pain is localized at the limb stump (reviewed in 5). According to a study by Buchheit and colleagues who examined data of 124 military service members who suffered traumatic amputation injury, 58% reported phantom pain and 61% residual limb pain. In 48,7% of those with residual pain, the cause was reported to be sensitized neuroma[6].

Apart from amputations, neuromas can also develop as a result of peripheral nerve trauma caused by lacerations, and crush or stretch injuries, compression or poorly performed neurorrhaphy of nerve transections[7]. Macroscopically, neuromas are benign neural tumors consisting of nerve fibers entangled in fibrotic tissue[8,9]. While the macroscopic and histological appearance of neuromas has been well characterized, the signaling mechanisms and development pathways underlying their formation and how this relates to neuropathic pain remains poorly understood[10].

2.2 Pathogenesis of neuromas

After nerve injury, a cascade of processes occurs, orchestrated by endocrine and paracrine signaling that begins with Wallerian degeneration, and is followed by axonal sprouting, that reconstructs nerve continuity and restores nerve function (reviewed in 11,12). These processes are governed by coordinated gene expression of various growth factors, cytokines, transcription factors, neuropeptides,

myelin proteins, cytoskeletal proteins as well as components of extracellular matrix[13–15]. When the distance between two severed nerve segments is large, or there is no distal end, as is the case with amputations, axon regrowth occurs in an unorganized pattern[16]. In these cases simultaneous proliferation of wound-repair cells and signaling molecules can lead to collagen remodeling and scar formation that form poorly vascularized, dense fibrous structures, known as neuromas[10].

It is thought that in the pathogenesis of neuroma formation, factors similar to those involved in nerve regeneration, play a major role. For instance, Nerve Growth Factor (NGF), whose role in nerve regeneration has been widely studied, is also implicated in neuroma formation. This was demonstrated by Kryger, et al. in a rat sciatic nerve model, in which the authors showed that inhibition of NGF reduces neuroma formation and neuropathic pain[17]. In another study, using the same model, Marcol, et al. showed that suppressing the effect of Brain Derived Nerve Factor (BDNF) led to similar results, however, high concentrations of BDNF increased the development of neuroma and neuropathic pain[18].

2.3 Histological characteristics of neuromas

Histologically, neuromas caused by trauma can be characterized as non-encapsulated, non-neoplastic conglomerates of cells and axons embedded in a dense fibrotic matrix[19,20]. Some studies and case reports have described traumatic neuromas presenting tangled morphology, composed of connective tissue, Schwann cells, and regenerating axons[21–23]. Inflammatory signaling factors[23] and myofibroblasts[24] have also been identified in painful neuromas. While microscopic features of fully formed neuroma have been well documented, little information exists about the cellular structure of neuromas in their early stages of development, from the time of nerve injury through to complete tumor formation. This information could be used to develop new and better treatments that target the early stages of neuroma development that potentially could prevent the associated pain.

2.4 Current treatments for neuroma-induced pain

Many treatment options exist for neuroma-induced pain. Pharmacological treatments include N-methyl-D-aspartate (NMDA) receptor antagonists, opioids, anticonvulsants, antidepressants, local anesthetics, and calcitonin, which act by inhibiting pain-signaling pathways. When using these treatments, chronic and adverse effects, and route of administration must be taken into consideration (reviewed in 5). Neuroma-induced pain can also be treated by surgical excision, however, of more than 150 different techniques described in the literature, none give lasting definitive pain relief, and at best may result in satisfactory results[25]. Surgical strategies used to treat neuromas range from targeted nerve implantation[26], nerve wrapping with collagen[27], vein implantation[28] and trans-positioning into muscles[29] or bones[30]. One of many surgical treatments that has received a great deal of attention is traction neurectomy. This consists of excising the affected nerve, while in traction, as high in the limb as possible, in order to place the distal nerve stump outside the zone of mechanical irritation and scarring[31]. Economides et al. showed that compared to traction neurectomy, combining various techniques resulted in better pain relief[32]. While some of these surgical methods, or their combination, have shown varying degrees of success, in general, existing treatments remain unsatisfactory, and most patients continue to suffer with this condition (reviewed in 33). It is with this in mind that we embarked upon this study to try to better understand how neuromas form in the first place.

In limb amputations, irrespective of the cause, nerve transection with resulting neuroma formation, is always present. This is due to the fact that after nerve transection, regenerating axons, in the proximal cut nerve, lack the distal nerve segment to guide their growth to restore nerve continuity. However, the presence of a neuroma does not always lead to pain. It is estimated that around 11 – 31% of lower extremity amputees suffer from neuroma-induced pain[34–36]. While the exact mechanisms involved in neuroma-induced pain are poorly understood it is hypothesized that two main mechanisms are involved. The first is overstimulation of free axonal endings in the zone of injury, with involvement of A delta and C fibers conveying the painful stimuli to the cortical somatosensory areas. These free axonal

endings present spontaneous electrical activity, with accompanying activity in the nerve bodies in the dorsal root ganglions[37]. The second mechanism is related to processes taking place in the somatosensory cortex that cause intensification of pain response secondary to peripheral nerve injury[37].

2.5 EStim treatment of neuroma-induced pain

Signal transmission, in the form of action potentials, is based on electrical changes in axons, with voltage-gated channels in the axolemma being a key component in this process (reviewed in 38). Many investigators have targeted the electrical properties of peripheral nerves, with the goal of stimulating nerve regeneration and thus reducing neuropathic pain[39–43]. There is increasing evidence that transcutaneous electrical nerve stimulation (TENS) may be effective in the treatment of neuropathic pain and/or promoting nerve regeneration. The effectiveness of this approach has been shown to be largely dependent on the frequency, intensity, and duration of the EStim as well as the location of electrodes and other factors[39,44]. Most of these studies have used devices that deliver EStim externally, through the skin. In contrast, in the present study, we treated the amputated limb stump using a surgically implanted device whose electrodes delivered EStim directly into the stump tissues.

2.6 Aims of the study

This study was designed to define and classify the early histological stages of nerve regrowth and neuroma formation following an amputation injury. In a rat limb amputation model, we used histological and immunohistochemical (IHC) analysis to characterize nerve regrowth and neuroma formation at different time points from the time of injury to full neuroma formation. Identifying and characterizing the different stages of neuroma development may provide helpful information in developing strategies to target new and improved treatments that could help alleviate pain and suffering in millions of patients worldwide.

In a previous study, our research group investigated the effects of low voltage direct current EStim on limb regeneration in a rat limb amputation model. While the

primary focus of that study was to evaluate the effects of EStim on new bone, cartilage and vessel formation, it was also noticed that in EStim treated animals there was less neuroma formation[45]. These unexpected results led us to investigate and quantitatively evaluate the effect of direct current EStim on neuroma formation in the same rat limb amputation model.

3. Materials and Methods

3.1 Study design

All animal experiments were performed in accordance with guidelines established by our animal care and oversight committee at the Johann Wolfgang Goethe-University in Frankfurt/Main, Germany and were approved by the Veterinary Department of the Regional Council in Darmstadt, Germany (Regierungspräsidium Darmstadt, Veterinärdezernat, Wilhelminenstraße 1–3) (Project No. FU 1114) in accordance with German law.

Overall, right forelimbs of 42 male Sprague Dawley rats were amputated. Nerve regrowth and neuroma formation were assessed in the stumps of amputated limbs of 30 male Sprague Dawley rats (Charles River Labs Int., Germany) (age = 5 weeks; weight = 100± 150g) at 3, 7, 28, 60 and 90 days after surgery (n = 6 per each timepoint) using histological and immunohistochemistry analysis.

Additionally, the effects of EStim on neuroma formation, 28 days post-amputation, was assessed in limb stumps treated with: 1) EStim (active device, n = 6), 2) no EStim (inactive device – sham, n = 6), and 3) no EStim (no device – control, n = 6). Animals with no implanted device whose limbs were harvested at 28 DPA were used both for the assessment of nerve regrowth and neuroma formation and as controls for evaluation of the effect of EStim on neuroma formation. The allocation of animals into the different groups is shown in Table 1.

Initially, the plan was to evaluate the effects of EStim at days 60 and 90, as well as at 28 days, however, due to problems with the implanted EStim devices, EStim delivery was not reliable at these latter time points. Most likely, this problem was technical and arose due to growth of the animals, causing damage and/or dislocation of the EStim device electrodes.

Table 1: Allocation of animals in groups

Day post amputation	No EStim No device	No EStim Deactivated device (sham)	EStim Active device
3	6		
7	6		
28	6	6	6
60	6		
90	6		

3.2 EStim device

Electrical stimulation in the form of direct current (DC) was applied to rat limb stumps using the same device as used in a previous study[45]. Briefly, it consisted of platinum and silver electrodes (Junker-Edelmetalle, Germany), measuring 1,3 cm and 3 cm in length, respectively, and 0,15 mm in diameter. The wires were welded to a 10 MΩ resistor on one end leaving the other end free (Fig. 1). Delivery of EStim was confirmed via direct measurements at the site of delivery with a precision multimeter. The electrical device generated 5 – 15nA of electrical current. In order for the EStim devices to withstand mechanical forces, we reinforced the weld between the resistor and the wires with a flexible plastic tube. The contact surface of the plastic tube and the wires was glued with quick drying, 2-component epoxy resin glue (UHU, Germany) and the whole length of the plastic tube and the resin glue was isolated and protected with medical grade silicone (RTV-coating Dow Corning, USA). Only 5 mm of silver wire (loop) and 10 mm of platinum wire was left exposed. In the sham group a 2,5 cm long piece of looped silver wire served as the "inactive" device. The devices were sterilized by immersion in 95% ethanol for 1 hour followed by 1-hour exposure to UV light, then washed with sterile PBS solution (Sigma-Aldrich, Germany), prior to implantation.
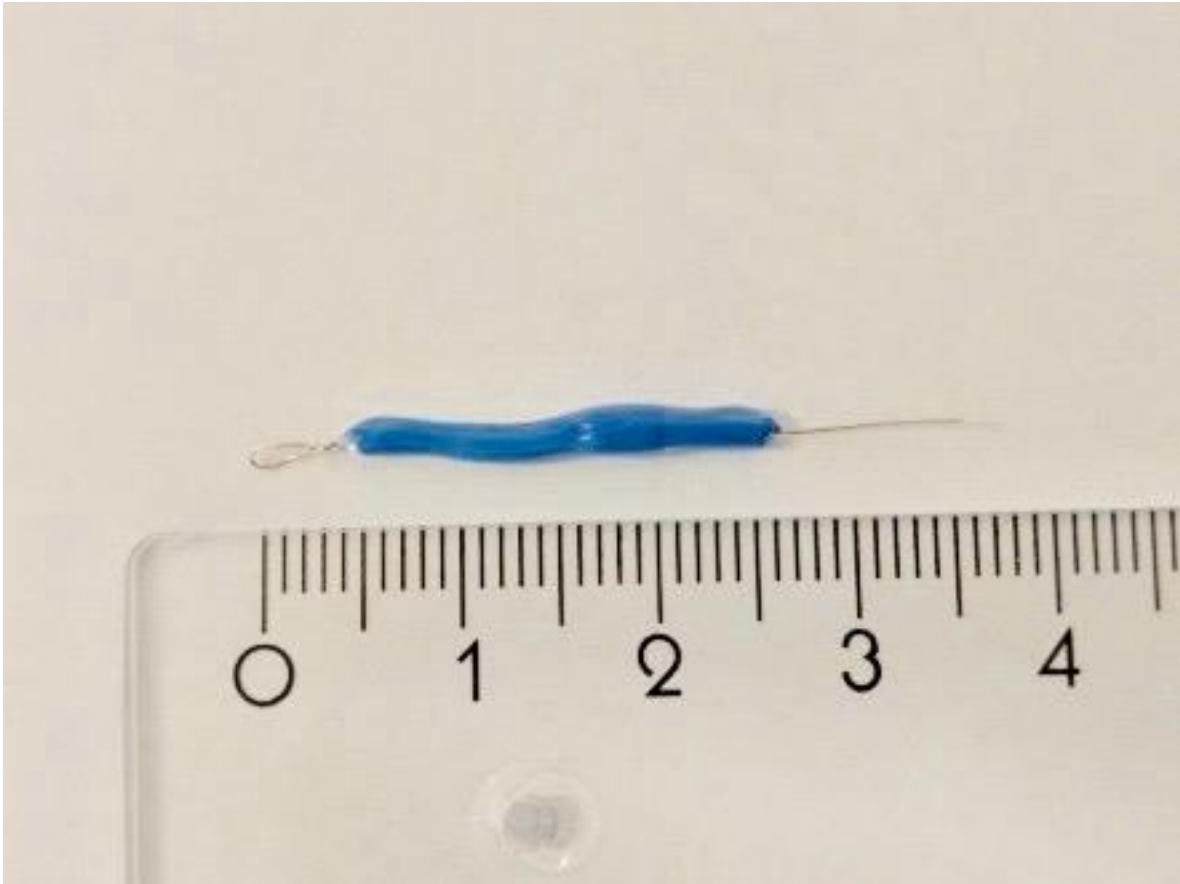
Figure 1. EStim device. Platinum electrode (right), silver electrode (loop), protective tube covering resistor (not visible), transparent silicon-coating leaving only the electrode tips exposed.

3.3 Limb amputation and EStim device implantation

While under intraperitoneal general anesthesia (Ketamine/Xylazine 100 mg/10 mg/kg body weight [BW]) the right limbs of the rats were shaved and cleaned with antiseptic fluid (Fig. 2A). Under aseptic conditions a circumferential skin incision was performed at the border of the middle and distal third of the right humerus. Using a microscope, microinstruments and 10-0 non-resorbable monofilament sutures (Ethicon, USA) the brachial artery and vein were identified, dissected free from the surrounding nerves, ligated and cut (Fig. 2B). Then, the soft tissue with the peripheral nerves were transected down to the humerus. The

humerus bone was then exposed and cut just distal to the deltoid tuberosity, using a gigli wire saw (Fig. 2C).

In the animals receiving EStim the "active" device was placed in a tunnel created in the deltoid muscle, the tip of the platinum wire electrode was bent and inserted approximately 2 mm into the medullary cavity of the humerus bone at the amputation site, and the silver wire electrode was fixed with a suture to the deltoid fascia (Fig. 2D). In the animals in the sham group, a silver wire (inactive device) was placed and fixed in the same way, while the control animals did not receive any device. In all 3 groups the skin was closed over the limb stump with a continuous intradermal suture (4-0 Vicryl, Ethicon, USA) and all animals received antibiotics (0,2 ml procaine penicillin containing 60.000 U) via intraperitoneal injection postoperatively. After surgery animals were monitored until they recovered from anesthesia, and then daily for complications or signs of pain and discomfort. Analgesia (Carprofen - 0,35 mg/100g BW) was administered subcutaneously on postoperative day one, and orally via the animals' drinking water (Tramadol - 2,5 mg/100ml), for 5 days thereafter.

Animals were housed in separate cages for two days postoperatively, then in groups of 4, in common cages, in a light (12-hour light – 12- hour dark), temperature (20–24° C) and airflow controlled room, and were given free access to food and water. Animals were euthanized (CO_2 inhalation) at 3, 7, 28, 60 and 90 days post amputation. The limb stumps were collected and examined macro- and microscopically for signs of infection or tumors. The limb stump specimens were fixed in 1x Zinc-Formal-Fixx, (Thermo scientific, USA) for 24 hours, decalcified for 14 days at 37 degrees Celsius in a 10% EDTA (Ethylenediaminetetraacetic acid) solution and 34 g/liter of Trizma base (Sigma), paraffin embedded and stored for subsequent histomorphometric and immunohistological analysis.
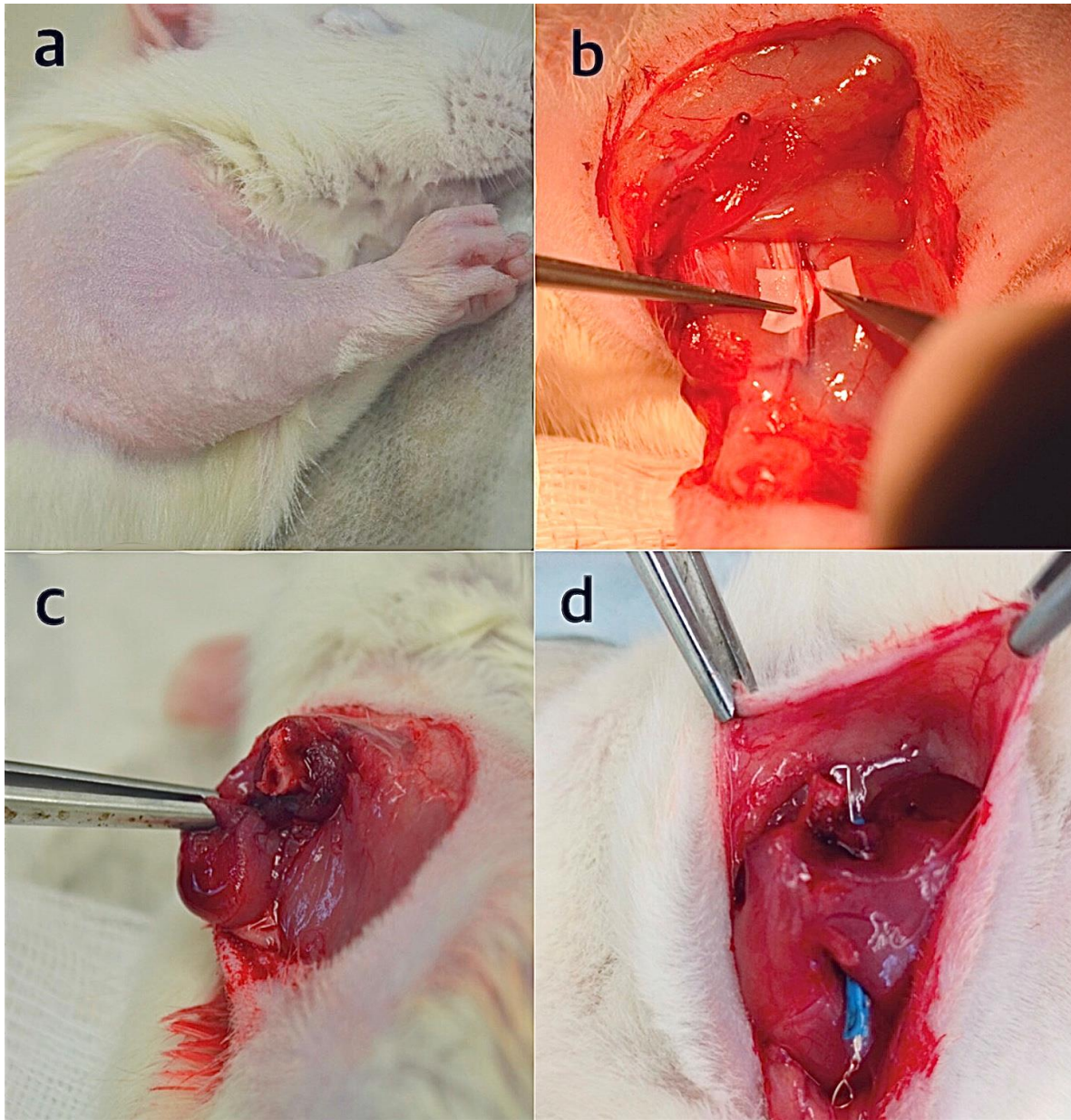
Figure 2: Forelimb amputation. Shaved and disinfected rat right forelimb (A), dissection and ligation of brachial artery and vein after skin incision and transection of the ventral brachial musculature (B), right forelimb after amputation, with exposed humerus and surrounding muscles before device implantation and skin closure (C), EStim device in-situ with the tip of the platinum electrode introduced into the medullary cavity of the humerus (middle top part of photo) and silver wire electrode loop fixed in adjacent shoulder muscles with resorbable suture (D).

3.4 Histology and immunohistochemistry

After decalcification, limb stumps were embedded in paraffin blocks, and longitudinal sections (5 µm thick) were cut with a Microtome (Leica RM2235, Leica, Germany) and mounted on glass microscope slides.

General morphology: Stump tissues from each time point were stained (Alcian Blue/Orange G-Hematoxilin-Eosin (AB&OG)) for morphological analysis[46], as described elsewhere[45]. Evaluation of nerve structures was performed using light microscopy (Ti-E, Nikon GmbH, Germany) and image analysis software (NIS-Elements 4.4, Nikon GmbH, Germany).

Immunohistochemistry (IHC): To assess nerve regrowth in limb stumps by IHC, heat antigen retrieval was performed in Citrate Buffer (DAKO, Germany) for 10 minutes. After blocking with 7% goat serum solution (DAKO, Germany), specimens were incubated with monoclonal mouse anti-human Neurofilament protein antibody (Clone 2F11, culture supernatant, 1:100; DAKO, Germany), which served as a marker for axons. For signal detection, EnVision + System-HRP (AEC) kit (DAKO, Germany) was used according to the manufacturer´s instructions. Finally, a counterstain with hematoxylin was performed and stained samples were viewed using light microscopy (Ti-E, Nikon GmbH, Germany). Morphological observations and quantitative evaluations were performed using image analysis software (NIS-Elements 4.4, Nikon GmbH, Germany). To assure that positive stain was not caused by non-specific interactions of immunoglobulin molecules, isotype controls were carried out in representative samples.

3.5 Histological evaluation parameters

Six limb stumps for each time point were analyzed and after careful examination, representative sections from each stump were taken for detailed evaluation. The selected stump sections were assessed from the humerus head to the most distal area of the amputated stump, thus, assuring observation and analysis across the entire stump section (Fig. 3A).

At each time point a qualitative scoring system was used in which the presence and location of nerves was recorded as either positive or negative by NF labeling (Fig.3B). Axonal density was measured to differentiate normal and degenerating axons. First, the total area (region of interest - ROI) to be analyzed was selected, then using a threshold tool to highlight NF positive stain in the ROI, a value for the stained area was assigned. Axonal density was calculated as the area of stained axons in the fascicles divided by the total area in the ROI. In each sample, 2-3 fascicles and/or bundles detected in the stump section, were measured at 20x magnification. Then mean values of axonal density of normal and degenerating axons, in each animal, were obtained for all time points.
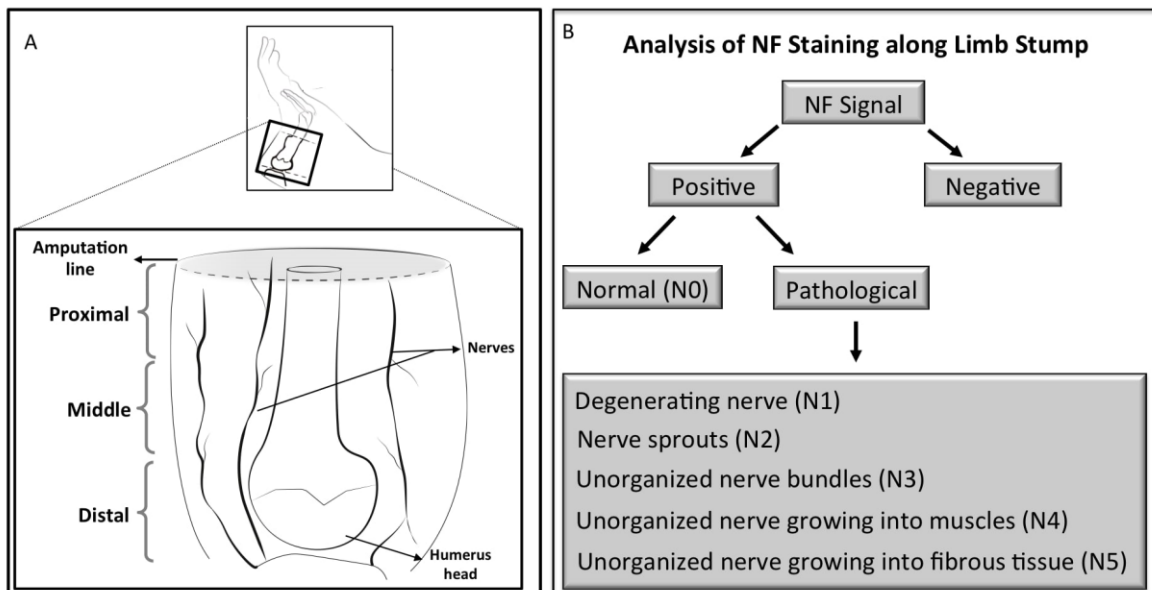
Figure 3: Schematic of amputation site and parameters analyzed. (A) Representative areas of the rat limb and stump samples collected for analysis. (B) Schematic description of parameters analyzed.

The contrast between normal and pathological axonal distribution was determined by careful examination of the relation between nerve fascicles and axons and the surrounding tissues at different time points. The different axonal morphological structures were classified into 6 different categories: Normal nerves-N0; Degenerating axons-N1; Axonal sprouts-N2; Unorganized bundles into

22

connective tissue-N3; Unorganized axons into muscles-N4; and Unorganized axons into fibrotic tissue-N5. Then their location in the limb stump was cataloged in all samples for each time point (Fig. 3B).

3.6 Assessing the effect of EStim on neuroma formation

Morphological features of peripheral nerves were evaluated in EStim (n=6), sham (n=6) and control (n=6) stumps at 28 days after amputation, as described above. Upon collection of the samples, the EStim devices (active and inactive) were carefully removed prior to fixing the tissues in formalin. The presence of the particular morphological features N0 to N5 was documented for all groups to allow for their comparison.

3.7 Statistical analysis

Differences of axonal density in normal and degenerating axons at the different time points were analyzed by Wilcoxon Signed-Rank Test using Graphpad Prism software ($p \leq 0.05$). Bootstrap of the data from percentage of animals affected by each feature at each time point was performed with 1000 repetitions using R-Studio platform for R-software and 95% confidence intervals (95% CI) were later calculated.

For the analysis of the occurrence of different histological nerve types in the limb stumps of EStim, Sham and Control group Fisher exact test was applied. The significance level was set at $\alpha = 0.05$. Statistical analysis was performed using BiAS for Windows[TM] version 11.10 software.

4. Results

4.1 Histological characteristics of peripheral nerves

All limb stumps were sectioned longitudinally, along the long axis of the limb, to maximize the area to observe nerve regrowth and neuroma formation. Intact peripheral nerves within muscle and connective tissue were observed in all stumps, at all time points. Limb stumps were examined and the 6 morphological categories were assigned by observation of overlapping AB&OG and NF-stained sections. AB&OG stained axon fascicles appeared light pink in color, surrounded by a light-colored brown membrane (perineurium) (Fig 4). Individual axons could only be identified at 20x magnification appearing as darker pink colored dots or sprouts. Detailed focal labeling of axons was clearly visible and readily distinguishable using immunohistochemistry with specific antibodies targeting neurofilament protein (NF) (Fig. 5). Higher values of axonal density were observed in fascicles with normal characteristics compared to degenerating axons at all the time points. Statistical analysis revealed significant differences between normal and degenerating axons at all time points, except 28 DPA (p≤0.05). Low numbers of nerves were measured in 28-day samples, which could have affected the precision of the statistical comparisons (Fig. 6).

4.1.1 Description of six distinct nerve characteristics

Great variability of nerve morphological features was observed with the most relevant listed in the predetermined 6 separate categories (Fig. 7). Due to the high variability in the position and orientation of the re-growing nerves in the limb stumps, sections contained nerves dissected longitudinally and transversely (Fig 7N0i and 7N0ii).

N0 - Normal nerves; when oriented longitudinally, appeared as neatly structured axons running along myelin sheaths, while when sectioned transversally appeared as a ring-like structures formed by compacted axon fibers surrounded by

connective tissue forming a neural membrane (Fig. 7N0i and 7N0ii). Normal nerves observed in tissue sections appeared to arise from branches of the main nerves of the brachial plexus.

N1 - Degenerating axons; were identified in nerve fascicles with lower density of NF signal in their structure (Fig. 7N1).

N2 - Axonal sprouts; appeared as delicate and sometimes isolated neurofilaments that looked like donut-rings or fine fibrils within the tissue (Fig. 7N2). More precisely, axons showing positive signal met the following criteria; not exceeding a maximum of 8-10 stripes or dots within an area of 200 μm^2, not arranged in bundle-like structures and located a minimum of 100 μm distance from a large nerve branch.

N3 - Unorganized axonal features; consisted of unorganized bundles of axons incorporated in connective tissue, histologically appearing as zones with many axonal fascicles of distinct size and orientation (Fig. 7N3);

N4 - Unorganized axons growing into muscle; appeared as small bundles of disorganized axons trapped in muscle (Fig. 7N4), usually located in the middle area of the stump tissue, adjacent to the bone,

N5 - Tangled axon fascicles embedded in fibrous tissue; corresponded to a classical neuroma[20,45,47] in late stages of development (Fig. 7N5).
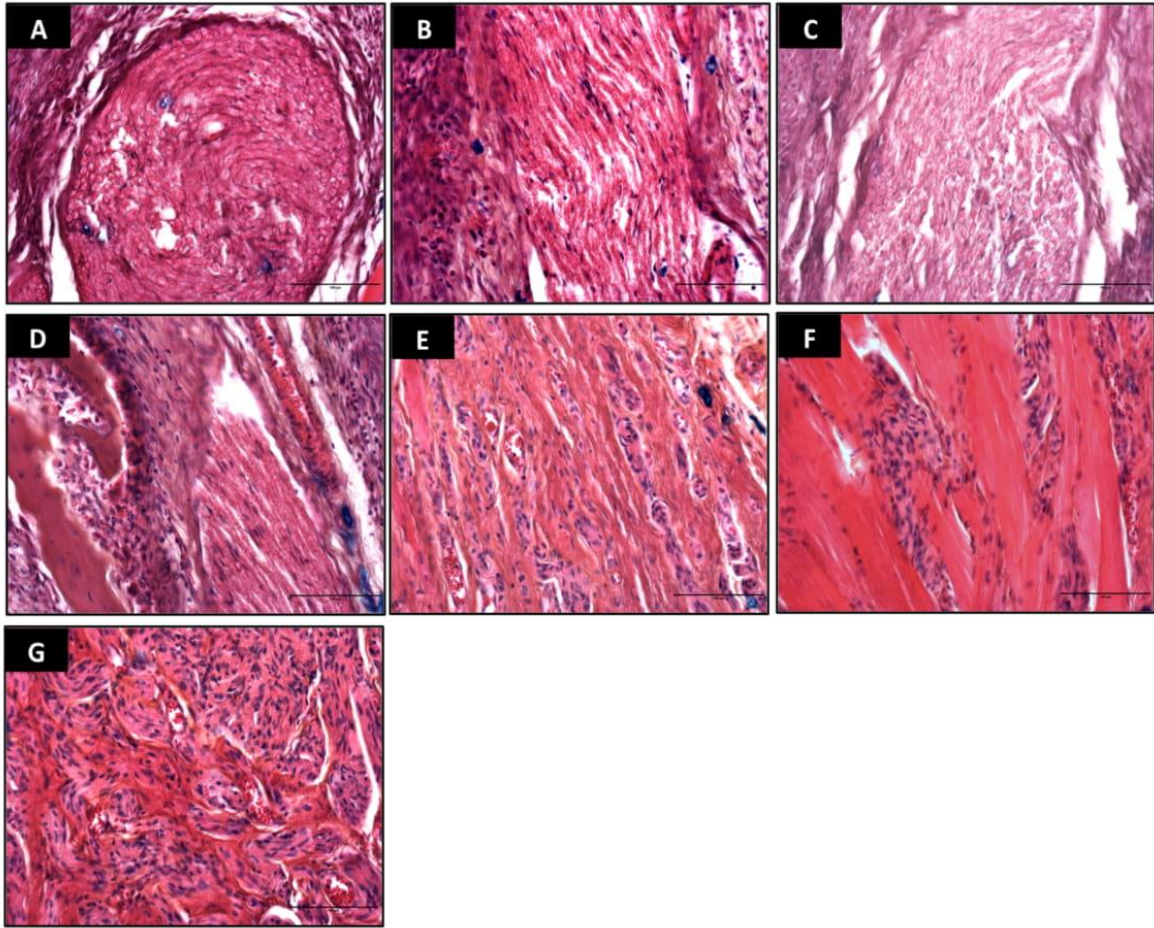
Figure 4: Representative images of peripheral nerve morphology in right forelimb stump tissue - stained with AB&OG. (A, B, C and D) Longitudinally and transversally cut nerve brunches demonstrating normal features (N0), degenerating axons (N1) and/or axonal sprouts (N2). Nerves with advanced pathological features: (E) unorganized axons bundled in connective tissue (N3), (F) unorganized axon ramifications in muscle (N4) and (G) neuroma-highly unorganized axons in tissue (N5). All images are 20x magnification with the scale bar = 100 µm.
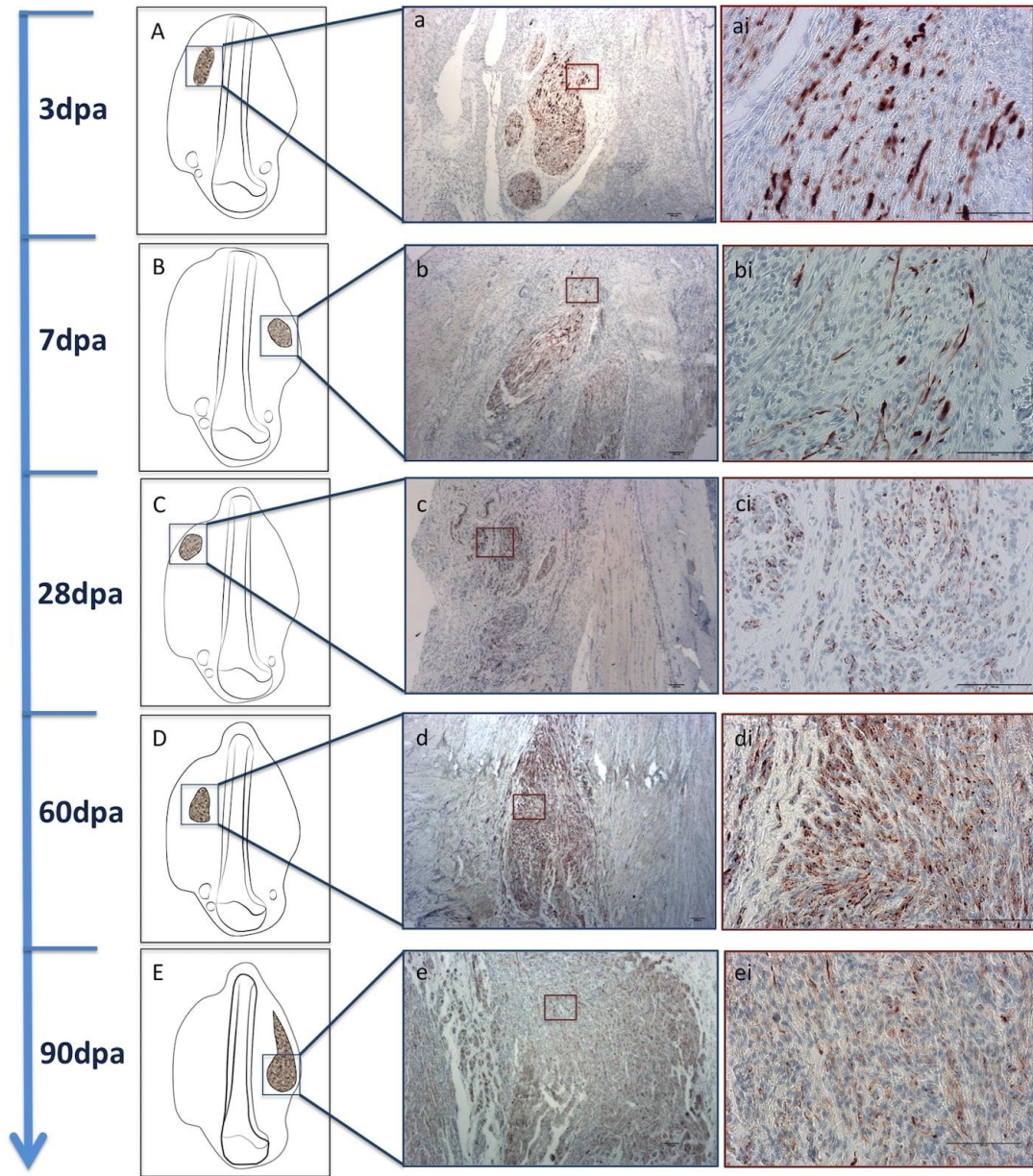
Figure 5: Nerve regrowth and neuroma development in limb stump tissues from days 3 through 90 - NF staining. (A, B, C, D and E) Schematic figures representing an overview of the location of the structures and representative images of axonal fascicles at higher magnification view (a, b, c, d and e with 4x magnification; ai, bi, ci, di and ei at 20x magnification, scale bar = 100μm) of structures over time.
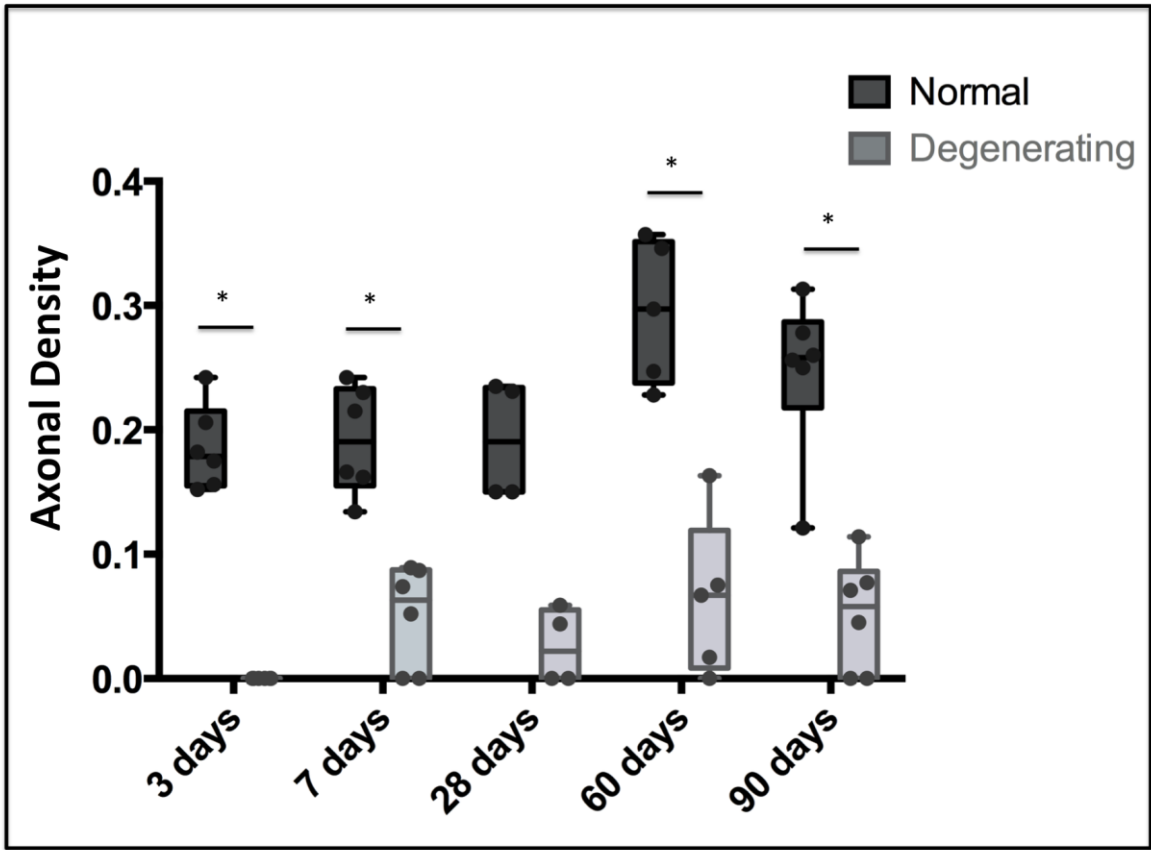
Figure 6: Axonal density of normal and degenerating nerves. Boxplot overlaid with sample distribution of axonal density of normal and degenerating axons. * Statistically significant differences (p≤0.05).
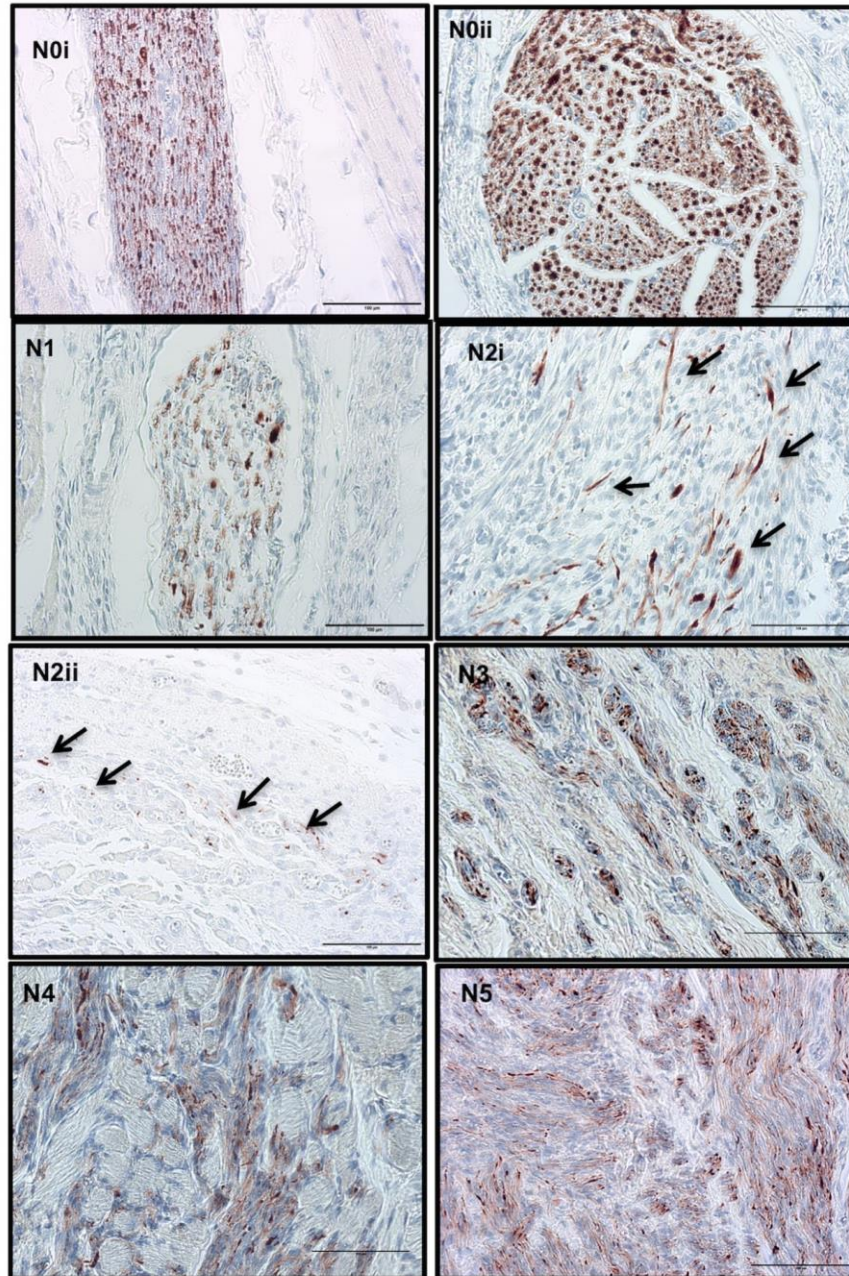
Figure 7: Nerve histology in rat limb stumps after amputation. Normal nerve (N0i: longitudinal and N0ii: transversal section), degenerating axons (N1), axonal sprouts (N2i: at the end of damaged fascicles, arrows show elongated structures corresponding to axonal fibers and N2ii: in the distal area, arrows show isolated axons appearing as donut ring-like structures), unorganized axons bundled in connective tissue (N3), unorganized axon ramifications in muscle (N4), neuroma-highly unorganized axons in tissue (N5). Scale bar = 100µm.

## 4.1.2 Histology of nerve characteristics over time

Degenerating axons (N1) were present in different areas of the tissue sections, first appearing at day 7, in approximately 60% of samples, then their number decreased at 28 days, and again increased at days 60 and 90. Axons in the N2 category (axonal sprouts) were visible in 60% and 100% of samples at day 3, and 7 respectively, and at later time points became less evident (Fig. 8). Unorganized features started to appear at 28 days post-amputation, where 33% of the samples presented axons in N3 and N4 stages, while 66% already revealed N5 stage. A similar pattern was observed at 60 days although the incidence of N3, N4, and N5 stages increased at day 90 when 100% of samples showed axonal fascicles in N5 stage. The distribution of morphological characteristics at each time point is shown in Fig. 8 and is described in detail below when discussing each time point.

In samples in the early stages after amputation (3 and 7 days) nerve branches from the brachial plexus appeared mainly normal, distributed along the long axis of the limb from proximal to distal areas. In some samples it was even possible to visualize complete fascicles of ulnar, median and/or radial nerves running the entire length of the stump from the humeral head to the distal zones.

In some 3-day samples, where nerve fibers were sectioned, signs of axonal sprouting were already visible in the middle and distal areas (Fig. 7N2i), and at 7 days, 100% of the samples had this appearance. Samples collected at 3 days did not reveal nerve fascicles with lower axonal density (axonal degeneration) in the distal area (closer to injured areas), however the majority of 7-day samples did (Fig. 8). Confidence intervals (95% CI) of bootstrapped data varied in very low range indicating a small possible range in the prevalence of the features analyzed.

Twenty-eight days after limb amputation, all 6 nerve characteristics of interest appeared in stump tissues. Nerve fascicles with normal and degeneration characteristics (N0 and N1) showed no significant difference in axonal density values. Apart from these fascicles, axonal sprouts, especially in the distal area, appeared like doughnut-ring structures (N2) (Fig. 7N2ii). Also, from this time point, zones of unorganized axonal growth were visible along the tissue stump (N3, N4 and N5). Twenty-eight-day samples revealed unorganized growth of axonal fibers

surrounding normal appearing nerve fascicles. This correlated with zones of nerve enlargement in fascicles sectioned longitudinally. Moreover, in the same amputated limb, variability of axonal characteristics and neuroma formation was detected throughout the stump tissue and in zones that anatomically correlated with areas of ulnar, median, radial and musculocutaneous nerve fibers.
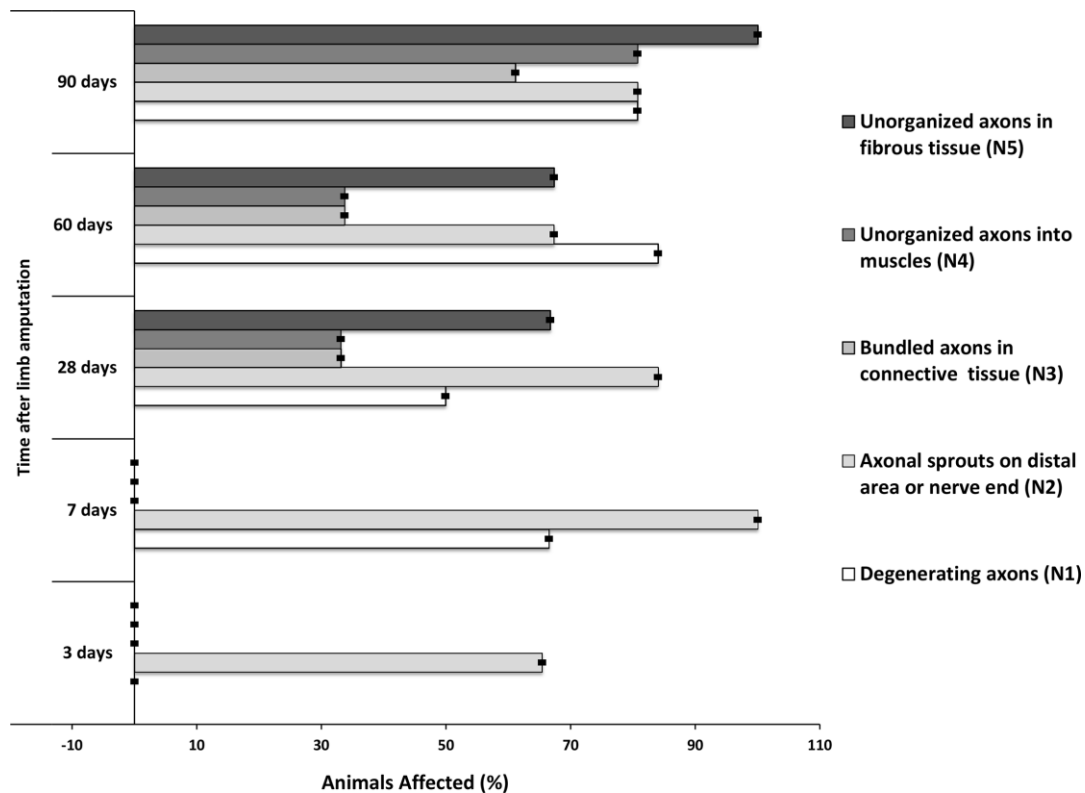
Figure 8: Nerve morphology in rat limb stumps at all measurement time points. Error bars represent confidence interval of 95%.

At days 60 and 90 normal appearing nerves were present in all samples, although gradually less evident and only present in the most proximal areas of the stump, closer to the trunks of nerves originated from the brachial plexus. The incidence of degenerating nerves was higher at days 60 and 90 compared to earlier time points (7 and 28 days). Sixty- and 90-day stump tissue contained unorganized bundled axons and fully formed neuromas, which were more evident and prevalent than in 28-day samples. Despite no differences in axonal density among neuromas

31

at the different time points, at 90 days abundant growth of unorganized axons into conjunctive and muscle tissue was visible.

4.2 Effect of EStim on neuroma inhibition

Morphological characteristics were evaluated in limb stump tissue at 28 days after amputation, and the results are summarized in Fig. 9 and Table 2. Each individual morphological characteristic was documented for each group (EStim, sham and control) as present or absent and the comparison for each of the morphological types (N1 – N5) was made. Evaluation of the occurrence of neuroma revealed the following: of the 6 rats with active EStim devices, one had neuroma (16,6%), while in sham (inactive devices), and control (no device) animals neuroma were present in 4 cases (66,6%). The difference was not significant with p value = 0.28. The unorganized axons in connective tissue (N3) and in muscle (N4) could be documented in 2 animals in the Control group, in 4 (N3) and 1 (N4) animals in the Sham group and in 2 (N3) and 0 (N4) rats in the EStim Group. Axonal sprouts (N2) were seen in 5 rats of the Control and Sham groups and 6 rats of the EStim group, while degenerating axons (N1) were seen in 3 rats of the Control group, all 6 Sham animals and 5 rats of the Estim group. The differences were not significant with p > 0,05.

Table 2: Nerve morphological types in limb stumps 28 days after amputation.

Morphological types	Control n=6	Sham n=6	EStim n=6	p value
Degenerating axons (N1)	3 (50%)	6 (100%)	5 (83,3%)	0,25
Axonal sprouts (N2)	5 (83,3%)	5 (83,3%)	6 (100%)	1,0
Unorganized bundled axons in connective tissue (N3)	2 (33,3%)	4 (66,6%)	2 (33,3%)	0,59
Unorganized axons in muscle tissue (N4)	2 (33,3%)	1 (16,6%)	0	0,74
Neuroma (N5)	4 (66,6%)	4 (66,6%)	1 (16,6%)	0,28
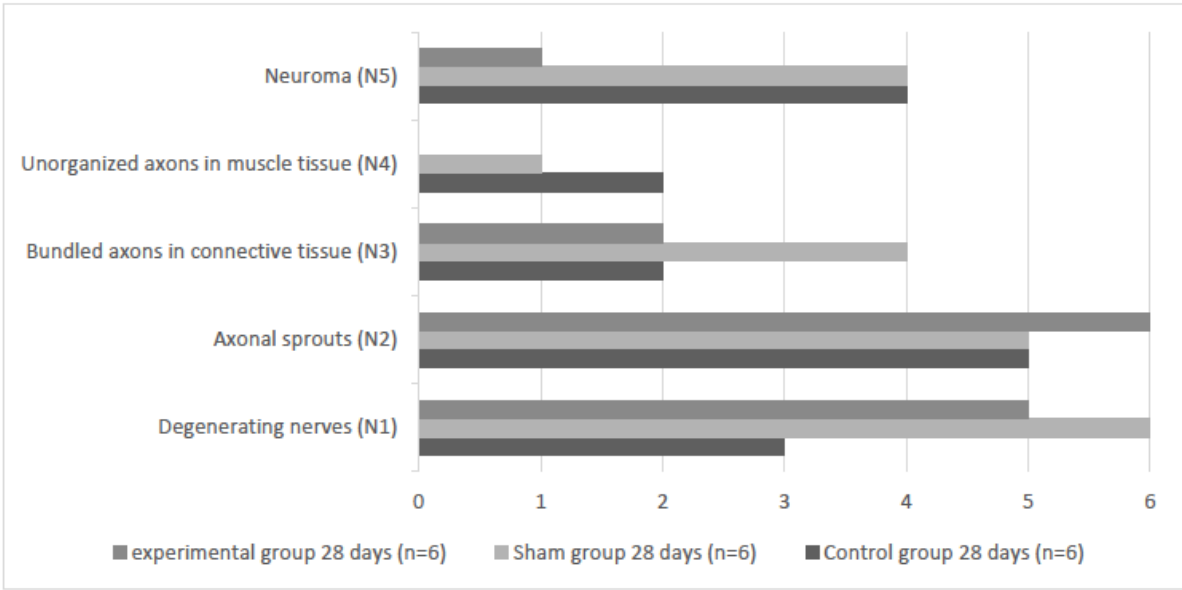
Figure 9: Nerve morphology 28 days after amputation in experimental, sham and control limb stump.

5. Discussion

5.1 Histological characteristics of peripheral nerves and neuroma development after limb amputation

Herein we document the progression of nerve regrowth and neuroma development from the time of injury for 90 days after amputation and analyze the effect of EStim on neuroma inhibition. Using IHC staining for neurofilament (NF) protein we were able to identify specific characteristics of axons and their relation with surrounding tissues throughout the 90-day period. Neurofilament proteins play important structural roles in neurons; together with microtubules and associated proteins, they sustain the axonal and dendritic branching patterns and promote axonal growth and thickening[48,49]. Variability of nerve patterns observed in our limb stump tissues over time could be correlated with different stages of nerve regrowth and neuroma development. Normal appearing nerve fascicles were visible in all sections analyzed, particularly at the early stages after amputation when their distribution in the stumps was near the site of injury. At later time points (60 and 90 days) normal appearing nerve fascicles were only visible at a distance from the injured stump tissue, near the humeral head.

Wallerian degeneration, which is essential for axon regeneration, starts hours after nerve injury with activation of phospholipases expressed in the Schwann cells and macrophages, that promote the removal of myelin and myelin-associated glycoproteins from the injured area (reviewed in 50,51). After debris clearing, growth factors are produced to stimulate Schwann cell migration and axonal regrowth (reviewed in 52). In this study, the presence of fascicles with less evident NF signal directly correlated with low axonal density, which was indicative of degenerating nerves in the stump tissues. Using epifluorescence microscopy, alterations at the axonal ultra-structure level have been reported in rat optical nerves already 30 minutes after injury[53]. Although the techniques used in the present study were not sensitive enough to detect alterations at this level, we did see degenerating axons

from day 7 on. Other models and/or microscopy techniques would have been necessary to identify these changes in nerve structures.

Intrinsic mechanisms involving calcium influx and activation of the protease Calpain are responsible for cytoskeletal degradation and axon degeneration (reviewed in 54). In addition, NF protein becomes sensitive to proteases when they are dephosphorylated (reviewed in 49). Nerve injury significantly increases the levels of dephosphorylated Nuclear Factor of Activated T-cells-DNFATc4[55]. Protection mechanisms against phosphatases have also been shown to play an important role in nerve regeneration[56,57]. The process of axonal degeneration has been observed not only in traumatic injuries, but also as a consequence of degenerative diseases. Despite the fact that the mechanism of this process is not fully understood, studies suggest similarities between both phenomena (reviewed in 54). Delayed axonal degeneration could also be associated with the expression of "Wallerian degeneration slow" (WldS) protein[58], impairment of Nmnat2 proteins in the cell body[59], and the absence of trophic signals to neurons[60]. In our study, degenerating axons seen in 90 DPA samples, might not be directly related to Wallerian degeneration that occurs immediately after injury. It may, however, be associated with other environmental factors. As a consequence of the lack of NF, deficiency in nerve regeneration can occur, although this may not be the result of neuronal death following injury[61].

Signs of axonal sprouts were visible at the site of amputation where the nerve was cut, already at day 3, and more so at day 7 post amputation. Spinal cord injuries initially present minimal axon degeneration, followed by nerve regeneration from the proximal axons towards the distal organ[62]. The axonal sprouts we saw early on could be attempts by axons to begin regenerating after Wallerian degeneration. Dun and Parkinson described transected mouse sciatic nerve axons that showed rapid axonal regrowth from day 4, leading to "misdirected axonal growth of 1.46 mm" on day 7[63]. Studies have shown that after injury, local growth factor and protein production support axonal growth and promotes nerve repair[15,64]. Although we did not measure protein levels, increased local protein production and the beginning of axonal

attempts to regenerate could have induced the sprout growth we observed in our IHC sections.

In this study we observed the first signs of neuroma formation at 28 days post amputation. Two modes of axonal growth in the early stages are suggested - elongation, in which axons advance fast and straight, and - branching, in which numerous small lateral outgrowths are formed[62]. Both elongated and branching structures were visible in our stump tissue at days 3 and 7. At 28 days we observed abnormal bulbous shaped axonal structures growing into muscle and/or fibrotic tissue. In the absence of a guiding structure, the signals that induce directed axon growth persist and instead of regrowing in an organized directional pattern, regenerating axons may regrow in unorganized patterns and form neuroma (reviewed in 65). In our samples, neuroma formation was detected already at 28 days, and became more evident and widespread at later time points (60 and 90 days).

In 28- and 60-day stumps areas of unorganized axonal structures were observed side-by-side with normal fascicles. Literature describes cases of segmented nerve injury whereby axons from the proximal end of a severed nerve regrow towards the distal end through tunnel-like structures formed by Schwann cells[62]. Since in our amputation limb model the distal nerve segment is missing, Schwann cells are not able to form tunnels to guide the axons, resulting in unorganized nerve regrowth. Thus, the neuromas that we observed in stump tissue at 28 DPA could have been caused by the absence of these Schwann cell tunnels and signaling, in which case attempts to communicate with the target organ to establish axonal recovery did not occur.

In parallel with nerve signaling and attempts to regrow, fibrotic tissue is formed in order to repair and close the wound. It is hypothesized that during axonal regrowth regenerating nerve fibers and associated connective tissue extend into regions at the same time that severely damaged tissue is in a proliferative phase of healing. When blocked by fibrotic tissue, the regenerating neural axons form spirals and end discs and become irregularly dispersed throughout the connective tissue[10]. The histologic changes we observed in our stump tissues over time are consistent

with the above-described hypothesis for neuroma formation, proposed by Foltán et al. (2008). Growth of regenerative nerve fibers into connective tissue is represented in our N3 stage samples, while nerve regrowth into muscle tissue corresponds to our N4 stage samples. Finally, axons blocked by fibrotic tissues forming massive chaotic structures, i.e. neuroma, corresponds to the N5 stage of our scale.

Neuroma caused by injury, or traumatic neuroma, are frequently characterized by massive tumors showing irregular arrangement of nerve fascicles within a collagenous and fibroblastic stroma[21,66–69]. Moreover, these lesions frequently present incomplete encapsulation and a mix of axons and Schwann cells[20]. These diagnostic descriptions of neuroma coincide with our N5 stage (unorganized axonal growth into fibrotic tissue) classification of fully formed neuroma.

Detailed histological analysis of symptomatic and asymptomatic neuromas has shown that fascicle number and diameter and nerve tissue density cannot be used to distinguish between painful and non-painful neuromas[67]. Histological signs of chronic inflammation have been shown to be associated with painful neuromas[21]. However, pain and abnormal sensitivity can also occur in the absence of inflammation. Even though our study did not necessarily focus on "painful" neuromas, we frequently observed unorganized nerve regrowth into connective tissue and muscle. Weng et al, identified the expression of alpha smooth muscle actin (α-SMA) in painful neuromas[66,70]. Alfa-SMA is a phenotypic marker for myofibroblast activity, which contributes to increased contractile activity of myofibroblasts[71]. Based on this it is conceivable that myofibroblast activity potentiate the development of painful neuroma.

The histological characteristics we observed in this study; unorganized axon bundles, axonal ingrowth into muscles and fibrous tissue, could be the manifestation of different stages of neuroma formation. We observed that axon regrowth starts already 3 days after amputation and by 28 days neuroma formation is clearly visible in many different nerves present in the stump tissue. Signals for axonal regrowth appear to be activated at 60 and 90 days. Moreover, in this study, where there was no intervention to prevent neuroma formation in the animals at 60 and 90 days after

amputation, neuroma formation occurred in 66,6 and 100% of the cases, respectively.

Our findings indicate that 28 days is a critical time point at which neuroma formation already occurs. Based on this perhaps treatment focused on inhibiting neuroma development should be initiated prior to this critical time point when growth is still dynamic and can be influenced. Future research will focus on studying the underlying mechanisms during this early time period in order to target specific factors that influence neuroma formation in the dynamic early stages of development. This could lead to new and better treatments and/or prevention strategies.

5.2 Effect of EStim on neuroma formation

The therapy algorithm of patients with limb pain after amputation is complex and requires a multidisciplinary approach[72]. EStim has been used as one of many treatment modalities for both residual as well as phantom limb pain. Both non-invasive and invasive forms of treatment have been tried. The most common non-invasive form of EStim therapy for neuroma-induced limb pain has been transcutaneous electrical nerve stimulation (TENS)[73]. While some studies report the effectiveness of TENS for the treatment of phantom and residual limb pain[74,75], its analgesic effect has yet to be confirmed in randomized controlled clinical trials[76].

Invasive EStim treatments, that require surgical implantation of devices include spinal cord stimulation (SCS)[77] and peripheral nerve stimulation (PNS)[78]. PNS has shown promising results mainly when used to treat chronic pain[79]. The exact mechanisms by which PNS exerts this effect is not well understood, however it is thought to alleviate pain by affecting membrane action potentials and is called the "gate control theory"[79,80]. Our results showed that only 1 of the 6 EStim treated animals developed neuromas at 28 days post-amputation. In contrast in the animals that did not receive EStim (controls and sham) 4 out of 6 developed neuromas. While our statistical analysis did not reveal a significant difference between these groups, due to large variations and small sample size, these findings are certainly suggestive of EStim having an effect.

A major drawback in these experiments was the technical difficulties we encountered with the implanted EStim devices. While we were able to confirm that the devices delivered EStim during the first 28 days, (via measuring functionality when they were explanted at 28 days), we could not confirm functionality at the 60 and 90 day post amputation time points. We believe that this technical problem arose due to growth of the animals, i.e. the growth of their limb stumps outgrew the implanted device electrodes. Therefore, at these later time points (60 and 90 DPA), we did not measure the effects of EStim on growth of unorganized axonal bundles in connective or muscle tissue. Had we been able to do so, as was originally planned, it is possible that neuroma formation would have been less present.

While our results seem generally promising, we were not able to confirm the effectiveness of EStim on the neuroma inhibition, in these experiments. To do so further research will be needed.

6. Conclusion

Six distinct morphological characteristics of peripheral nerve regrowth and neuroma formation were measured 3, 7, 28, 60 and 90 days after limb amputation in a rat model. Neuroma formation was apparent starting at 28 days after amputation in the majority of animals. From our findings we believe that this early, dynamic phase of neuroma formation should be explored as a possible target for inhibiting neuroma formation. Based on our findings, it appears that EStim, delivered directly to the tissues containing affected nerves, might be a good candidate as a possible therapeutic approach for reducing neuroma formation. Future studies will focus on mechanisms by which EStim affects neuroma formation in the first 28 days post-amputation, how EStim affects pain-inducing versus non-symptomatic neuromas in the first 28 days post-amputation, and best methods for preventing neuroma formation in the first 28 days post-amputation.

7. References

1. Ziegler-Graham K, MacKenzie EJ, Ephraim PL, Travison TG, Brookmeyer R. Estimating the Prevalence of Limb Loss in the United States: 2005 to 2050. *Arch Phys Med Rehabil*. 2008;89(3):422-429. doi:10.1016/j.apmr.2007.11.005

2. Dillingham TR, Pezzin LE, MacKenzie EJ. Limb amputation and limb deficiency: epidemiology and recent trends in the United States. *South Med J*. 2002;95(8):875-883. doi:10.1097/00007611-200208000-00018

3. Hisam A, Ashraf F, Rana MN, Waqar Y, Karim S, Irfan F. Health Related Quality of Life in Patients with Single Lower Limb Amputation. *J Coll Physicians Surg Pak*. 2016;26(10):851-854. doi:2456

4. Horgan O, MacLachlan M. Psychosocial adjustment to lower-limb amputation: a review. *Disabil Rehabil*. 26(14-15):837-850. http://www.ncbi.nlm.nih.gov/pubmed/15497913. Accessed September 22, 2019.

5. Hsu E, Cohen SP. Postamputation pain: epidemiology, mechanisms, and treatment. *J Pain Res*. 2013;6:121-136. doi:10.2147/JPR.S32299

6. Buchheit T, Van de Ven T, Hsia H-LJ, et al. Pain Phenotypes and Associated Clinical Risk Factors Following Traumatic Amputation: Results from Veterans Integrated Pain Evaluation Research (VIPER). *Pain Med*. 2016;17(1):149-161. doi:10.1111/pme.12848

7. Rajput K, Reddy S, Shankar H. Painful Neuromas. *Clin J Pain*. 2012;28(7):639-645. doi:10.1097/AJP.0b013e31823d30a2

8. Watson J, Gonzalez M, Romero A, Kerns J. Neuromas of the Hand and Upper Extremity. *J Hand Surg Am*. 2010;35(3):499-510. doi:10.1016/j.jhsa.2009.12.019

9. Mackinnon SE, Dellon AL. Results of treatment of recurrent dorsoradial wrist neuromas. *Ann Plast Surg*. 1987;19(1):54-61. doi:10.1097/00000637-198707000-00009

10. Foltán R, Klíma K, Špačková J, Šedý J. Mechanism of traumatic neuroma

development. *Med Hypotheses*. 2008;71(4):572-576.
doi:10.1016/j.mehy.2008.05.010

11. Wood MD, Mackinnon SE. Pathways regulating modality-specific axonal regeneration in peripheral nerve. *Exp Neurol*. 2015;265:171-175. doi:10.1016/j.expneurol.2015.02.001

12. Namgung U. The role of Schwann cell-axon interaction in peripheral nerve regeneration. *Cells Tissues Organs*. 2014;200(1):6-12. doi:10.1159/000370324

13. Yamauchi J, Chan JR, Shooter EM. Neurotrophins regulate Schwann cell migration by activating divergent signaling pathways dependent on Rho GTPases. *Proc Natl Acad Sci U S A*. 2004;101(23):8774-8779. doi:10.1073/pnas.0402795101

14. Michalski B, Bain JR, Fahnestock M. Long-term changes in neurotrophic factor expression in distal nerve stump following denervation and reinnervation with motor or sensory nerve. *J Neurochem*. 2008;105(4):1244-1252. doi:10.1111/j.1471-4159.2008.05224.x

15. Gillen C, Korfhage C, Müller HW. ■ REVIEW : Gene Expression in Nerve Regeneration. *Neurosci*. 1997;3(2):112-122. doi:10.1177/107385849700300210

16. Yüksel F, Kişlaoğlu E, Durak N, Uçar C, Karacaoğlu E. Prevention of painful neuromas by epineural ligatures, flaps and grafts. *Br J Plast Surg*. 1997;50(3):182-185. doi:10.1016/s0007-1226(97)91367-9

17. Kryger GS, Kryger Z, Zhang F, Shelton DL, Lineaweaver WC, Buncke HJ. Nerve growth factor inhibition prevents traumatic neuroma formation in the rat. *J Hand Surg Am*. 2001;26(4):635-644. doi:10.1053/jhsu.2001.26035

18. Marcol W, Kotulska K, Larysz-Brysz M, Kowalik JL. BDNF contributes to animal model neuropathic pain after peripheral nerve transection. *Neurosurg Rev*. 2007;30(3):235-243; discussion 243. doi:10.1007/s10143-007-0085-5

19. Rainsbury JW, Whiteside OJH, Bottrill ID. Traumatic facial nerve neuroma following mastoid surgery: a case report and literature review. *J Laryngol Otol*. 2007;121(6):601-605. doi:10.1017/S0022215106004993

20. Argenyi ZB. Immunohistochemical characterization of palisaded, encapsulated neuroma. *J Cutan Pathol*. 1990;17(6):329-335. doi:10.1111/j.1600-0560.1990.tb00108.x

21. Hirose T, Tani T, Shimada T, Ishizawa K, Shimada S, Sano T. Immunohistochemical demonstration of EMA/Glut1-positive perineurial cells and CD34-positive fibroblastic cells in peripheral nerve sheath tumors. *Mod Pathol*. 2003;16(4):293-298. doi:10.1097/01.MP.0000062654.83617.B7

22. Egami S, Tanese K, Honda H, Kasai H, Yokoyama T, Sugiura M. Traumatic neuroma on the digital tip: Immunohistochemical analysis of inflammatory signaling pathways. *J Dermatol*. 2016;43(7):836-837. doi:10.1111/1346-8138.13297

23. Khan J, Noboru N, Young A, Thomas D. Pro and anti-inflammatory cytokine levels (TNF-α, IL-1β, IL-6 and IL-10) in rat model of neuroma. *Pathophysiol Off J Int Soc Pathophysiol*. 2017;24(3):155-159. doi:10.1016/j.pathophys.2017.04.001

24. Yan H, Zhang F, Kolkin J, Wang C, Xia Z, Fan C. Mechanisms of nerve capping technique in prevention of painful neuroma formation. Price TJ, ed. *PLoS One*. 2014;9(4):e93973. doi:10.1371/journal.pone.0093973

25. Elliot D. Surgical management of painful peripheral nerves. *Clin Plast Surg*. 2014;41(3):589-613. doi:10.1016/j.cps.2014.03.004

26. Pet MA, Ko JH, Friedly JL, Mourad PD, Smith DG. Does targeted nerve implantation reduce neuroma pain in amputees? *Clin Orthop Relat Res*. 2014;472(10):2991-3001. doi:10.1007/s11999-014-3602-1

27. Thomsen L, Schlur C. [Incidence of painful neuroma after end-to-end nerve suture wrapped into a collagen conduit. A prospective study of 185 cases]. *Chir Main*. 2013;32(5):335-340. doi:10.1016/j.main.2013.07.001

28. Mobbs RJ, Vonau M, Blum P. Treatment of painful peripheral neuroma by vein implantation. *J Clin Neurosci*. 2003;10(3):338-339. http://www.ncbi.nlm.nih.gov/pubmed/12763341. Accessed September 26, 2019.

29. Ay S, Akinci M. Primary transposition of digital nerves into muscle in second

ray amputation: a possible answer for neuroma formation. *Tech Hand Up Extrem Surg.* 2003;7(3):114-118. http://www.ncbi.nlm.nih.gov/pubmed/16518229. Accessed September 26, 2019.

30. Mass DP, Ciano MC, Tortosa R, Newmeyer WL, Kilgore ES. Treatment of Painful Hand Neuromas by Their Transfer into Bone. *Plast Reconstr Surg.* 1984;74(2):182-185. doi:10.1097/00006534-198408000-00002

31. Tintle SM, Donohue MA, Shawen S, Forsberg JA, Potter BK. Proximal Sural Traction Neurectomy During Transtibial Amputations. *J Orthop Trauma.* 2012;26(2):123-126. doi:10.1097/BOT.0b013e318214fd7b

32. Economides JM, DeFazio M V, Attinger CE, Barbour JR. Prevention of Painful Neuroma and Phantom Limb Pain After Transfemoral Amputations Through Concomitant Nerve Coaptation and Collagen Nerve Wrapping. *Neurosurgery.* 2016;79(3):508-513. doi:10.1227/NEU.0000000000001313

33. Yao C, Zhou X, Zhao B, Sun C, Poonit K, Yan H. Treatments of traumatic neuropathic pain: a systematic review. *Oncotarget.* 2017;8(34):57670-57679. doi:10.18632/oncotarget.16917

34. Tintle SM, Shawen SB, Forsberg JA, et al. Reoperation After Combat-Related Major Lower Extremity Amputations. *J Orthop Trauma.* 2014;28(4):232-237. doi:10.1097/BOT.0b013e3182a53130

35. Ebrahimzadeh MH, Hariri S. Long-term outcomes of unilateral transtibial amputations. *Mil Med.* 2009;174(6):593-597. doi:10.7205/milmed-d-02-8907

36. Ebrahimzadeh MH, Fattahi AS. Long-term clinical outcomes of Iranian veterans with unilateral transfemoral amputation. *Disabil Rehabil.* 2009;31(22):1873-1877. doi:10.1080/09638280902810968

37. Torebjörk E. Human microneurography and intraneural microstimulation in the study of neuropathic pain. *Muscle Nerve.* 1993;16(10):1063-1065. doi:10.1002/mus.880161010

38. Debanne D, Campanac E, Bialowas A, Carlier E, Alcaraz G. Axon physiology. *Physiol Rev.* 2011;91(2):555-602. doi:10.1152/physrev.00048.2009

39. Gordon T, Udina E, Verge VMK, de Chaves EIP. Brief electrical stimulation accelerates axon regeneration in the peripheral nervous system and promotes sensory axon regeneration in the central nervous system. *Motor Control.* 2009;13(4):412-441. http://www.ncbi.nlm.nih.gov/pubmed/20014648. Accessed September 29, 2019.

40. King EW, Audette K, Athman GA, Nguyen HOX, Sluka KA, Fairbanks CA. Transcutaneous electrical nerve stimulation activates peripherally located alpha-2A adrenergic receptors. *Pain.* 2005;115(3):364-373. doi:10.1016/j.pain.2005.03.027

41. DeSantana JM, Walsh DM, Vance C, Rakel BA, Sluka KA. Effectiveness of transcutaneous electrical nerve stimulation for treatment of hyperalgesia and pain. *Curr Rheumatol Rep.* 2008;10(6):492-499. http://www.ncbi.nlm.nih.gov/pubmed/19007541. Accessed September 29, 2019.

42. Aarskog R, Johnson MI, Demmink JH, et al. Is mechanical pain threshold after transcutaneous electrical nerve stimulation (TENS) increased locally and unilaterally? A randomized placebo-controlled trial in healthy subjects. *Physiother Res Int.* 2007;12(4):251-263. doi:10.1002/pri.384

43. Claydon LS, Chesterton LS, Barlas P, Sim J. Effects of simultaneous dual-site TENS stimulation on experimental pain. *Eur J Pain.* 2008;12(6):696-704. doi:10.1016/j.ejpain.2007.10.014

44. Chesterton LS, Foster NE, Wright CC, Baxter GD, Barlas P. Effects of TENS frequency, intensity and stimulation site parameter manipulation on pressure pain thresholds in healthy human subjects. *Pain.* 2003;106(1-2):73-80. doi:10.1016/s0304-3959(03)00292-6

45. Leppik LP, Froemel D, Slavici A, et al. Effects of electrical stimulation on rat limb regeneration, a new look at an old model. *Sci Rep.* 2015;5:18353. doi:10.1038/srep18353

46. Nowalk JR, Flick LM. Visualization of different tissues involved in endochondral ossification with alcian blue hematoxylin and orange G/eosin

counterstain. *J Histotechnol.* 2008;31(1):19-21. doi:10.1179/his.2008.31.1.19

47. Vora AR, Bodell SM, Loescher AR, Smith KG, Robinson PP, Boissonade FM. Inflammatory cell accumulation in traumatic neuromas of the human lingual nerve. *Arch Oral Biol.* 2007;52(1):74-82. doi:10.1016/j.archoralbio.2006.08.015

48. Helfand BT, Mendez MG, Pugh J, Delsert C, Goldman RD. A Role for Intermediate Filaments in Determining and Maintaining the Shape of Nerve Cells. *Mol Biol Cell.* 2003;14(12):5069-5081. doi:10.1091/mbc.E03-06-0376

49. Yuan A, Rao M V., Veeranna, Nixon RA. Neurofilaments and Neurofilament Proteins in Health and Disease. *Cold Spring Harb Perspect Biol.* 2017;9(4):a018309. doi:10.1101/cshperspect.a018309

50. Glenn TD, Talbot WS. Signals regulating myelination in peripheral nerves and the Schwann cell response to injury. *Curr Opin Neurobiol.* 2013;23(6):1041-1048. doi:10.1016/j.conb.2013.06.010

51. Faroni A, Mobasseri SA, Kingham PJ, Reid AJ. Peripheral nerve regeneration: experimental strategies and future perspectives. *Adv Drug Deliv Rev.* 2015;82-83:160-167. doi:10.1016/j.addr.2014.11.010

52. Gaudet AD, Popovich PG, Ramer MS. Wallerian degeneration: Gaining perspective on inflammatory events after peripheral nerve injury. *J Neuroinflammation.* 2011;8. doi:10.1186/1742-2094-8-110

53. Knöferle J, Koch JC, Ostendorf T, et al. Mechanisms of acute axonal degeneration in the optic nerve in vivo. *Proc Natl Acad Sci U S A.* 2010;107(13):6064-6069. doi:10.1073/pnas.0909794107

54. Wang JT, Medress ZA, Barres BA. Axon degeneration: Molecular mechanisms of a self-destruction pathway. *J Cell Biol.* 2012;196(1):7-18. doi:10.1083/jcb.201108111

55. Cai Y-Q, Chen S-R, Pan H-L. Upregulation of nuclear factor of activated T-cells by nerve injury contributes to development of neuropathic pain. *J Pharmacol Exp Ther.* 2013;345(1):161-168. doi:10.1124/jpet.112.202192

56. Mesfin MN, von Reyn CR, Mott RE, Putt ME, Meaney DF. In vitro stretch injury induces time- and severity-dependent alterations of STEP

phosphorylation and proteolysis in neurons. *J Neurotrauma*. 2012;29(10):1982-1998. doi:10.1089/neu.2011.2253

57. Abe N, Cavalli V. Nerve injury signaling. *Curr Opin Neurobiol*. 2008;18(3):276-283. doi:10.1016/j.conb.2008.06.005

58. Hoopfer ED, McLaughlin T, Watts RJ, Schuldiner O, O'Leary DDM, Luo L. Wlds protection distinguishes axon degeneration following injury from naturally occurring developmental pruning. *Neuron*. 2006;50(6):883-895. doi:10.1016/j.neuron.2006.05.013

59. Gilley J, Coleman MP. Endogenous Nmnat2 is an essential survival factor for maintenance of healthy axons. *PLoS Biol*. 2010;8(1):e1000300. doi:10.1371/journal.pbio.1000300

60. Nikolaev A, McLaughlin T, O'Leary DDM, Tessier-Lavigne M. APP binds DR6 to trigger axon pruning and neuron death via distinct caspases. *Nature*. 2009;457(7232):981-989. doi:10.1038/nature07767

61. Zhu Q, Couillard-Després S, Julien JP. Delayed maturation of regenerating myelinated axons in mice lacking neurofilaments. *Exp Neurol*. 1997;148(1):299-316. doi:10.1006/exnr.1997.6654

62. Kerschensteiner M, Schwab ME, Lichtman JW, Misgeld T. In vivo imaging of axonal degeneration and regeneration in the injured spinal cord. *Nat Med*. 2005;11(5):572-577. doi:10.1038/nm1229

63. Dun XP, Parkinson DB. Visualizing Peripheral nerve regeneration by whole mount staining. *PLoS One*. 2015;10(3). doi:10.1371/journal.pone.0119168

64. Verma P, Chierzi S, Codd AM, et al. Axonal protein synthesis and degradation are necessary for efficient growth cone regeneration. *J Neurosci*. 2005;25(2):331-342. doi:10.1523/JNEUROSCI.3073-04.2005

65. Wu D, Murashov AK. Molecular mechanisms of peripheral nerve regeneration: Emerging roles of microRNAs. *Front Physiol*. 2013;4 APR. doi:10.3389/fphys.2013.00055

66. Yan H, Gao W, Pan Z, Zhang F, Fan C. The expression of α-SMA in the painful traumatic neuroma: potential role in the pathobiology of neuropathic pain. *J Neurotrauma*. 2012;29(18):2791-2797. doi:10.1089/neu.2012.2502

67. Vora AR, Loescher AR, Craig GT, Boissonade FM, Robinson PP. A light microscopical study on the structure of traumatic neuromas of the human lingual nerve. *Oral Surg Oral Med Oral Pathol Oral Radiol Endod*. 2005;99(4):395-403. doi:10.1016/j.tripleo.2004.08.011

68. Mavrogenis AF, Pavlakis K, Stamatoukou A, et al. Current treatment concepts for neuromas-in-continuity. *Injury*. 2008;39 Suppl 3:S43-8. doi:10.1016/j.injury.2008.05.015

69. Kang J, Yang P, Zang Q, He X. Traumatic neuroma of the superficial peroneal nerve in a patient: a case report and review of the literature. *World J Surg Oncol*. 2016;14(1):242. doi:10.1186/s12957-016-0990-6

70. Weng W, Zhao B, Lin D, Gao W, Li Z, Yan H. Significance of alpha smooth muscle actin expression in traumatic painful neuromas: a pilot study in rats. *Sci Rep*. 2016;6:23828. doi:10.1038/srep23828

71. Hinz B, Celetta G, Tomasek JJ, Gabbiani G, Chaponnier C. Alpha-smooth muscle actin expression upregulates fibroblast contractile activity. *Mol Biol Cell*. 2001;12(9):2730-2741. doi:10.1091/mbc.12.9.2730

72. Subedi B, Grossberg GT. Phantom limb pain: Mechanisms and treatment approaches. *Pain Res Treat*. 2011;2011. doi:10.1155/2011/864605

73. Dubinsky RM, Miyasaki J. Assessment: Efficacy of transcutaneous electric nerve stimulation in the treatment of pain in neurologic disorders (an evidence-based review): Report of the therapeutics and technology assessment subcommittee of the American academy of neurology. *Neurology*. 2010;74(2):173-176. doi:10.1212/WNL.0b013e3181c918fc

74. Mulvey MR, Radford HE, Fawkner HJ, Hirst L, Neumann V, Johnson MI. Transcutaneous Electrical Nerve Stimulation for Phantom Pain and Stump Pain in Adult Amputees. *Pain Pract*. 2013;13(4):289-296. doi:10.1111/j.1533-2500.2012.00593.x

75. Katz J, Melzack R. Auricular transcutaneous electrical nerve stimulation (TENS) reduces phantom limb pain. *J Pain Symptom Manage*. 1991;6(2):73-83. doi:10.1016/0885-3924(91)90521-5

76. Johnson MI, Mulvey MR, Bagnall A-M. Transcutaneous electrical nerve

stimulation (TENS) for phantom pain and stump pain following amputation in adults. *Cochrane Database Syst Rev*. August 2015. doi:10.1002/14651858.CD007264.pub3

77.   Bunch JR, Goldstein H V., Hurley RW. Complete coverage of phantom limb and stump pain with constant current SCS system: A case report and review of the literature. *Pain Pract*. 2015;15(1):E20-E26. doi:10.1111/papr.12226

78.   Rauck RL, Kapural L, Cohen SP, et al. Peripheral Nerve Stimulation for the Treatment of Postamputation Pain-A Case Report. *Pain Pract*. 2012;12(8):649-655. doi:10.1111/j.1533-2500.2012.00552.x

79.   Nayak R, Banik RK. Current Innovations in Peripheral Nerve Stimulation. *Pain Res Treat*. 2018;2018. doi:10.1155/2018/9091216

80.   Soin A, Fang ZP, Velasco J. Peripheral neuromodulation to treat postamputation pain. *Prog Neurol Surg*. 2015;29:158-167. doi:10.1159/000434669

8. Appendix

8.1 Abbreviations

AB&OG	alcian blue/orange G-hematoxilin-eosin
BDNF	brain-derived neurotrophic factor
BW	body weight
CI	confidence interval
dpa	day post amputation
ECM	extracellular matrix
EDTA	ethylenediaminetetraacetic acid
ES/EStim	electrical stimulation
IHC	immunohistochemistry
kg BW	Kilogram body weight
nA	nano ampere
NF	neurofilament
PBS	phosphate-buffered saline
PNS	peripheral nerve stimulation
ROI	region of interest
SC	Schwann cell
SCS	spinal cord stimulation
TENS	transcutaneous electrical nerve stimulation
UV	ultraviolet
WldS protein	Wallerian degeneration slow protein

8.2 Acknowledgement

8.3 Curriculum vitae

Persönliche Daten

Name	Lukáš Pindur	Nationalität	Tschechische Republik
Geburtsdatum	07.09.1985,	Familienstand	verheiratet
Geburtsort	Český Těšín, Tschechische Republik		
E-Mail	lukas.pin85@gmail.com		

Universitäre Ausbildung

09/2005 - 05/2011	MUDr. (Medicinae Universae Doctor)	2. Medizinische Fakultät, Karls-Universität in Prag, Tschechische Republik

Beruflicher Werdegang

Seit 04/2017	Assistenzarzt	BGU Frankfurt am Main, Abteilung für Plastische, Hand- und Rekonstruktive Chirurgie
03/2016 – 03/2017	Research Fellow	Frankfurt Initiative for Regenerative Medicine, Goethe-Universität, Frankfurt, Deutschland
12/2015 - 01/2016	Visiting Surgeon	Department of Plastic Surgery, Chang Gung Memorial Hospital, Taipei, Taiwan
10/2014 - 10/2015	Assistenzarzt	Krankenhaus St. Barbara, Intensivstation, Schwandorf, Deutschland

10/2012 - 09/2014	Assistenzarzt	Klinikum St. Marien Amberg, Klinik für Allgemein-, Viszeral- und Thoraxchirurgie und Klinik für Unfallchirurgie und Orthopädie, Amberg, Deutschland
07/2011 - 09/2012	Assistenzarzt	Krankenhaus Trinec, Klinik für Allgemeinchirurgie und Unfallchirurgie und Klinik für Plastische Chirurgie, Trinec, Tschechische Republik

Publikationen

Perez-Abadia G, Janko M, **Pindur L**, et al. Frankfurt microsurgery course: the first 175 trainees. *Eur J Trauma Emerg Surg*. 2017;43(3):377-386.

Oliveira KMC, **Pindur L**, Han Z, Bhavsar MB, Barker JH, Leppik L. Time course of traumatic neuroma development. Blum R, ed. *PLoS One*. 2018;13(7):e0200548.

Leppik L, Zhihua H, Mobini S, Thottakkattumana P, Eischen-Loges M, Slavici A, Helbing J, **Pindur L**, Oliveira KMC, Bhavsar MB, Hudak L, Henrich D, Barker JH. Combining electrical stimulation and tissue engineering to treat large bone defects in a rat model. *Sci Rep*. 2018;8(1):6307.

Oliveira KMC, Barker JH, Berezikov E, **Pindur L**, Kynigopoulos S, Eischen-Loges M, Zhihua H, Bhavsar MB, Henrich D, Leppik L. Electrical stimulation shifts healing/scarring towards regeneration in a rat limb amputation model. *Sci Rep*. 2019;9(1):11433.

Sprachkenntnisse

Englisch	fließend	in Wort und Schrift
Deutsch	fließend	in Wort und Schrift
Tschechisch (Muttersprache)	fließend	in Wort und Schrift

8.4 Schriftliche Erklärung

Ich erkläre ehrenwörtlich, dass ich die dem Fachbereich Medizin der Johann Wolfgang Goethe-Universität Frankfurt am Main zur Promotionsprüfung eingereichte Dissertation mit dem Titel:

Time course of traumatic neuroma development/role of electrical stimulation in inhibition of neuroma formation in a rat limb amputation model

in der Orthopädischen Universitätsklinik Friedrichsheim unter Betreuung und Anleitung von Prof. Dr. med. John H. Barker mit Unterstützung durch Dr. Liudmila Leppik und Dr. Karla Mychellyne Costa Oliveira ohne sonstige Hilfe selbst durchgeführt und bei der Abfassung der Arbeit keine anderen als die in der Dissertation angeführten Hilfsmittel benutzt habe. Darüber hinaus versichere ich, nicht die Hilfe einer kommerziellen Promotionsvermittlung in Anspruch genommen zu haben.

Ich habe bisher an keiner in- oder ausländischen Universität ein Gesuch um Zulassung zur Promotion eingereicht. Die vorliegende Arbeit wurde bisher nicht als Dissertation eingereicht.

Vorliegende Ergebnisse der Arbeit wurden in folgendem Publikationsorgan veröffentlicht:
Oliveira KMC, Pindur L, Han Z, Bhavsar MB, Barker JH, Leppik L. Time course of traumatic neuroma development. PLoS One. 2018;13(7):e0200548.

_____   _____

          (Ort, Datum)   (Unterschrift)